entropy

MDPI

Article

Investigation of the Intra- and Inter-Limb Muscle Coordination of Hands-and-Knees Crawling in Human Adults by Means of Muscle Synergy Analysis

Xiang Chen [1,*], Xiaocong Niu [1], De Wu [2], Yi Yu [1] and Xu Zhang [1]

[1] Department of Electronic Science and Technology, University of Science and Technology of China (USTC), Hefei 230026, China; xcniu@mail.ustc.edu.cn (X.N.); yyu309@mail.ustc.edu.cn (Y.Y.); xuzhang90@ustc.edu.cn (X.Z.)

[2] Department of Pediatrics, the First Affiliated Hospital of Anhui Medical University, Hefei 230022, China; derk_wu@163.com

* Correspondence: xch@ustc.edu.cn; Tel.: +86-551-6360-1175

Academic Editors: Danilo P. Mandic, Andrzej Cichocki, Chung-Kang Peng and Kevin Knuth
Received: 27 March 2017; Accepted: 15 May 2017; Published: 17 May 2017

Abstract: To investigate the intra- and inter-limb muscle coordination mechanism of human hands-and-knees crawling by means of muscle synergy analysis, surface electromyographic (sEMG) signals of 20 human adults were collected bilaterally from 32 limb related muscles during crawling with hands and knees at different speeds. The nonnegative matrix factorization (NMF) algorithm was exerted on each limb to extract muscle synergies. The results showed that intra-limb coordination was relatively stable during human hands-and-knees crawling. Two synergies, one relating to the stance phase and the other relating to the swing phase, could be extracted from each limb during a crawling cycle. Synergy structures during different speeds kept good consistency, but the recruitment levels, durations, and phases of muscle synergies were adjusted to adapt the change of crawling speed. Furthermore, the ipsilateral phase lag (IPL) value which was used to depict the inter-limb coordination changed with crawling speed for most subjects, and subjects using the no-limb-pairing mode at low speed tended to adopt the trot-like mode or pace-like mode at high speed. The research results could be well explained by the two-level central pattern generator (CPG) model consisting of a half-center rhythm generator (RG) and a pattern formation (PF) circuit. This study sheds light on the underlying control mechanism of human crawling.

Keywords: surface EMG; muscle synergy; hands-and-knees crawling; two-level CPG

1. Introduction

Humans can crawl in several forms including hands-and-feet crawling, hands-and-knees crawling, creeping, scooting, and the combinations of different styles, among which hands-and-knees crawling is the most common [1,2]. For infants and young children, crawling is often regarded as one of their most important developmental milestones. Consequently, the understanding of the coordination between limbs, muscles, and joints during crawling and the underlying control mechanism of human crawling is meaningful for the assessment of motor development in the clinic.

Crawling is a kind of typical quadruped locomotion. In the past few years, many studies have been performed to investigate the inter-limb coordination of quadrupeds and primates in sports, and distinct inter-limb coordination patterns were observed during quadrupedal locomotion. In the studies of horses and primates, based on the stride interval between the footfalls of the fore-limb and hind-limb on the same side, Hildebrand defined inter-limb coordination into four patterns including diagonal-couplets, lateral-couplets, diagonal-sequence, and lateral-sequence [3,4]. He found

that short-legged animals often used the diagonal-couplets inter-limb coordination pattern whereas long-legged animals might use the lateral-couplets coordination pattern [5]. As for human crawling, Patrick et al. defined the phase lag between the initiation of stance of the left arm and the left leg as the ipsilateral phase lag (IPL) to quantify inter-limb coordination of crawling with hands and knees. According to the values of IPL, they classified inter-limb coordination into pace-like, trot-like, and no-limb-pairing patterns [6].

Since the 20th century, the study of inter-limb coordination during human crawling movement has attracted certain attention. In most related studies, crawling movements were monitored using video capture devices or kinematic sensors and the findings were often presented based on kinetic or kinematic data [6–9]. For instance, using camera and twin-axis electrogoniometers, Patrick et al. observed large variability and flexibility of limb coordination in adults but not in infants and suggested that this discrepancy resulted from the immaturity of the neuromuscular system of infants [6]. Using a 9-camera Vicon-612 system, Maclellan et al. found that healthy adults crawling on separate treadmills generally preserved a 1:1 frequency relationship between the arms and legs when the speeds of the arms and legs did not deviate from each other too much. When there was a large difference between the speeds of the arms and legs, an integer frequency ratio was maintained between the arms and legs [7]. The main drawback of studies based on kinetic or kinematic data is that only indirect evidence can be provided for the understanding of the neuromuscular control mechanism of crawling movement.

Surface electromyography is a potential tool in revealing central nervous system motor control strategies because it directly carries the neuromuscular control information. In particular, muscle synergy analysis based on sEMG signals has been verified to be a feasible tool to explore the coordination across muscles during movement. As one of the many hypotheses attempting to offer solutions or models that deal with the Degree of Freedom (DOF) problem of motion, muscle synergy was defined as a vector specifying a pattern of relative muscle activation. The absolute activation of muscle synergy was presumed to be modulated by a single neural command signal [10]. In the past few years, plenty of evidence has been reported to support the view that the central nervous system (CNS) might generate motor commands through a linear combination of a set of muscle synergies [11]. For instance, in the study of the frog kicking locomotion in different directions, D'Avella et al. suggested that the variety of behavioral goals could be explained by the combinations of a small number of muscle synergies [12]. Ting and Macpherson found that four muscle synergies in cats could reproduce multiple muscle activation patterns to keep balance under perturbations from different directions [13]. In particular, muscle synergy in human walking had been explored extensively [14–19]. Tang et al. compared the gait muscle synergies of cerebral palsy (CP) children, and typically developed children and adults, and found that the abnormalities of muscle synergy in CP children could reflect their motor dysfunction and even the physiological change in their nervous system [18]. Chia et al. found that rectilinear walking and curvilinear walking shared the same muscle synergies, but a fine-tuning in muscle synergies was introduced during curvilinear conditions, adapting the kinematic strategy to the new biomechanical needs [19].

Although considerable progress has been made toward human crawling, much less is known about the reason for the variety of inter-limb coordination. On the other hand, because crawling is a rhythmic movement consisting of periodic extension and flexion of four limbs, the muscle coordination with a single limb is also very meaningful for the understanding of the neuromuscular control mechanism of crawling movement. However, the current studies on crawling movement pay more attention to the inter-limb coordination, but the intra-limb muscle coordination is seldom involved. The novelty of this paper lies in the fact that muscle synergy analysis was applied firstly to human adult crawling with hands-and-knees. Specifically, the intra- and inter-limb muscle coordination in human hands-and-knees crawling movement were investigated from the perspective of muscle synergy. Considering the great potential in revealing the neuromuscular control strategy of muscle synergy analysis, the findings of this study are of great significance for understanding the underlying control mechanism of the CNS during crawling movement.

2. Materials and Methods

As shown in Figure 1, the research route of this study can be summarized as follows:

- Subjects were recruited to complete a number of hands-and-knees crawling experiments under different crawling speeds;
- Surface EMG signals were recorded from 32 main functional muscles of the subjects during the crawling task;
- Muscle synergies of four limbs were extracted respectively using the nonnegative matrix factorization (NMF) algorithm based on the sEMG data;
- Muscle synergies analysis under different conditions was conducted to explore the underlying control mechanism of human hands-and-knees crawling.

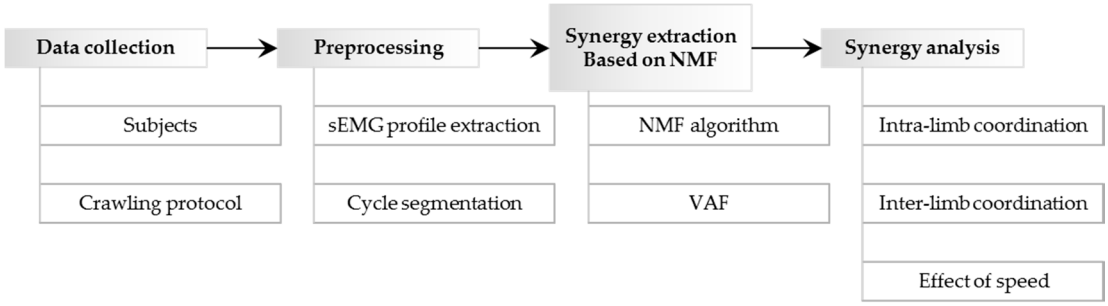

Figure 1. The research route of this study.

2.1. Subjects and Crawling Protocol

Twenty healthy subjects (15 males and 5 females, age (mean ± SD): 24.51 ± 0.76 years old, height: 174.10 ± 5.01 cm, weight: 58.43 ± 5.53 kg) without neurological or cardiovascular disorders participated in this study. None of the subjects had experienced serious injuries in the upper and lower limbs. All the participants were informed of the experimental procedure and signed an informed consent approved by the local Ethics Review Committee. The study was conducted in accordance with the Declaration of Helsinki.

In this study, the experiments were conducted on a treadmill (F63PRO; SOLE, Santa Barbara, CA, USA). The running belt of the treadmill is 1.5 m long and 0.6 m wide, and the adjustable speed range is from 1 km/h to 15 km/h. Because it was hard for most subjects to crawl more than 10 consecutive cycles at above 2.2 km/h, each subject was asked to perform four crawling trials at 1, 1.4, 1.8, and 2.2 km/h controlled speeds, respectively, on the running belt with 0° inclination. Participants need to complete at least 12 consecutive crawling cycles at each speed, and rest at least 2 min between two trials to avoid muscle fatigue. In addition, all subjects spent about half an hour to familiarize themselves with the treadmill and crawling tasks before the experiments.

2.2. Crawling Data Collection

Surface EMG signals of the 32 most relevant muscles were collected during the crawling task by means of a home-made multi-channel acquisition system. For each side of the body, 8 upper limb related muscles including flexor carpi radialis (FCR), flexor carpi ulnaris (FCU), extensor carpi ulnaris (ECU), extensor carpi radialis (ECR), biceps brachii(BIC), triceps brachii (TRIC), anterior deltoid (AD), latissimus dorsi (LD), and 8 lower limb muscles including rectus abdominis (RA), gluteus maximus (GM), iliopsoas (ILIO), vastus medialis (VM), rectus femoris (RF), vastus lateralis (VL), biceps femoris (BF), and semitendinosus (ST) were selected. Four flexors and four extensors were involved in each limb. In order to minimize the cross talk from adjacent muscles and optimize the valuable signals, electrodes were placed based on the guidelines of the Surface Electromyography for the Non-Invasive

Assessment of Muscles (SENIAM) protocol [20]. Surface EMG electrodes were attached to slightly shaved and cleaned skin above the muscle belly. Moreover, Acceleration (ACC) signals were collected by means of 3D accelerometers attached on the upper arm and thigh to calculate the phase lag between two given limbs (Figure 2). The *X* axis of each accelerometer was aimed at the forward direction. Surface EMG signals were amplified (×1000), and then sampled at 2000 Hz, while ACC signals were sampled at 100 Hz. In addition, before the experiment, each subject performed a series of maximal voluntary contraction (MVC) tasks to obtain MVC sEMG for each muscle. The design of the MVC task referred to the previous studies ([21,22] for arm muscles, [23] for trunk muscles, [24,25] for leg muscles). To prevent fatigue, MVC was performed on each muscle one by one, and there was enough time for each muscle to rest. All data was saved for offline analysis using Matlab 7.14.

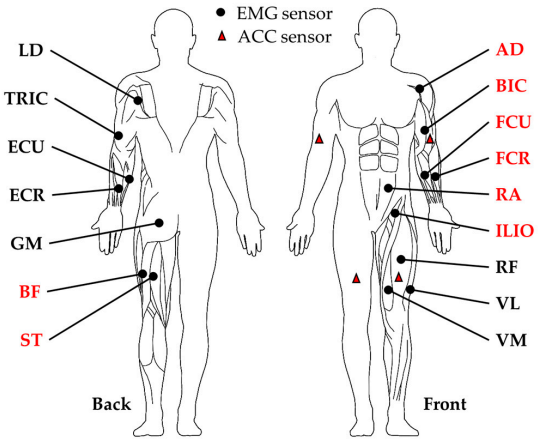

Figure 2. Placement of sEMG sensors and accelerometers. Red font means flexor and black font means extensor.

2.3. Surface EMG Profile Extraction and Cycle Segmentation

To extract the profiles, sEMG signals were high-pass filtered (zero-lag Butterworth filter with a cut-off of 20 Hz) firstly and then demeaned, rectified, and low-pass filtered (zero-lag Butterworth filter with a cut-off of 15 Hz). The extracted sEMG profile of each muscle was normalized to its maximum value obtained at the MVC task.

The crawling cycle was defined as the interval between two consecutive hits of the right palm to the ground. In this study, ACC signals of the *X* axis were used for the segmentation of crawling cycles. Since every hit was accompanied by a burst of acceleration of the right arm, the peaks of ACC signals were detected to mark the hits and identify the crawling cycles. To eliminate the disturbances of the beginning and the ending of a trail, the first and the last three cycles were discarded. The remaining cycles (no less than 6 cycles for each trail) were resampled into 500-point (T) for further data analysis.

2.4. Nonnegative Matrix Factorization Based Muscle Synergy Extraction

Muscle synergy analysis usually assumes that a muscle activation pattern is comprised of a linear combination of a few muscle synergies recruited by time-varying coefficients, and the recruitment coefficient represents the neural command that specifies how much a synergy contributes to one certain muscle's total activation. The NMF algorithm has been fully described by Lee and Seung [26] and used to extract muscle synergies in related studies [18,27]. As Equation (1) shows, NMF can decompose a non-negative sEMG profile matrix into a muscle synergy matrix *W* and a recruitment coefficient matrix *C*, and each muscle synergy in matrix *W* is considered to be functionally recruited by the corresponding coefficient vector in matrix *C*.

$$sEMG^{m \times n} = W^{m \times s} C^{s \times n} \quad (1)$$

In Equation (1), m is the number of muscles, n represents the length of the sEMG profile, and s means the number of extracted muscle synergies. In the process of factorization, W and C were initialized to be random values firstly and then updated using the updating rules [28]. When an original matrix *sEMGo* is decomposed into matrix W^* and C^* after multiple iterations, a reconstructed matrix *sEMGr* could be obtained by $sEMGr = W^*C^*$, and the variability accounted for (*VAF*, ranges from 0 to 1) [29] between *sEMGo* and *sEMGr* was calculated as Equation (2) to assess if the extracted muscle synergies could adequately reconstruct the original matrix. In this study, for each subject, c (>6) crawling cycles at each speed were selected for muscle synergy extraction. *VAF*s and the muscle synergy matrices were averaged across c cycles.

$$VAF = 1 - (sEMG_0 - sEMG_r)^2 / EMG_0^2 \tag{2}$$

2.5. Similarities between Muscle Synergy Structures and between Recruitment Patterns

The similarities of muscle synergies were estimated from the synergy structure (W) and recruitment pattern (C). For two muscle synergies ($W1$ ($C1$) and $W2$ ($C2$)), the structure similarity and recruitment pattern similarity were assessed by Pearson's correlation coefficient (r) as shown in Equations (3) and (4):

$$r_{W1\sim W2} = \frac{n\sum_{i=1}^{n} W1_i W2_i - \sum_{i=1}^{n} W1_i \sum_{i=1}^{n} W2_i}{\sqrt{n\sum_{i=1}^{n} W1_i{}^2 - \left(\sum_{i=1}^{n} W1_i\right)^2}\sqrt{n\sum_{i=1}^{n} W2_i{}^2 - \left(\sum_{i=1}^{n} W2_i\right)^2}} \tag{3}$$

$$r_{C1\sim C2} = \frac{m\sum_{i=1}^{m} C1_i C2_i - \sum_{i=1}^{m} C1_i \sum_{i=1}^{m} C2_i}{\sqrt{m\sum_{i=1}^{m} C1_i{}^2 - \left(\sum_{i=1}^{m} C1_i\right)^2}\sqrt{m\sum_{i=1}^{m} C2_i{}^2 - \left(\sum_{i=1}^{\mathrm{m}} C2_i\right)^2}} \tag{4}$$

2.6. Intra-Limb Muscle Coordination Analysis

In this study, sEMG profiles from eight muscles of each limb were decomposed using the NMF algorithm to extract muscle synergies and their corresponding recruitment patterns. Then the muscle synergies extracted from each limb were analyzed to explore the intra-limb muscle coordination during crawling movement. To explore the effect of crawling speed on the intra-limb muscle coordination, the structure similarity of the muscle synergies extracted at different speeds was analyzed. For two synergies with similar structure, the differences in their recruitment patterns were explored further. As shown in Figure 3, the effects of crawling speed on the recruitment patterns of two synergies with similar structure were evaluated from three aspects: recruitment level difference (Δp), recruitment phase lag (Δph), and recruitment time length difference (Δtl).

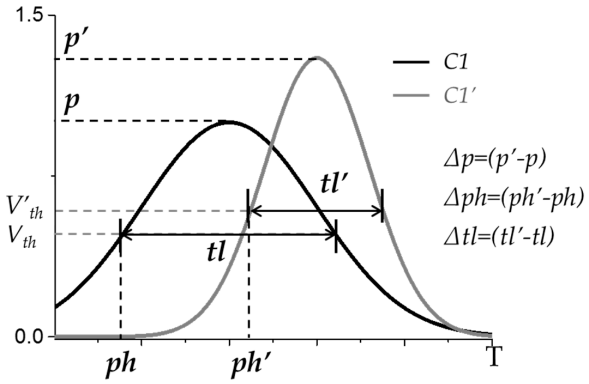

Figure 3. Evaluation parameters for two recruitment patterns (*C1*, *C1'*) of two synergies with similar structure. As in [17], V_{th} of each profile was set to the half-maximum value.

2.7. Inter-Limb Coordination Analysis

In order to quantify the inter-limb coordination, Patrick and his co-workers defined phase lags between certain limbs as the delay of the initiations of stance phases of corresponding limbs [6]. When initiation of the stance phase in the right leg occurred at a time interval "t1" after initiation of the stance phase in the right arm as shown in the top subgraph of Figure 4, ipsilateral phase lag (IPL) was defined as the ratio of t1 and T (a cycle duration). Similarly, contralateral phase lag (CPL) was expressed by dividing "t2" by T, and diagonal phased lag (DPL) was expressed by dividing "t3" by T. According to the above definitions, limb phase lags ranged from 0% to 100%. According to the IPL values, human crawling inter-limb coordination patterns were divided into trot-like patterns (IPL close to 50%, Figure 4, top subgraph), pace-like patterns (IPL close to 0% or 100%, Figure 4, bottom subgraph), and no-limb-pairing patterns (IPL between pace and trot, Figure 4, middle subgraph). For the no-limb-pairing pattern, IPL ranging from 10% to 40% means four-beat walks in the diagonal-sequence (right arm → right leg → left arm → left leg, DPL: 60–90%) and 60% to 90% means four-beat walks in the lateral-sequence (right arm → left leg → left arm → right leg, DPL: 10–40%).

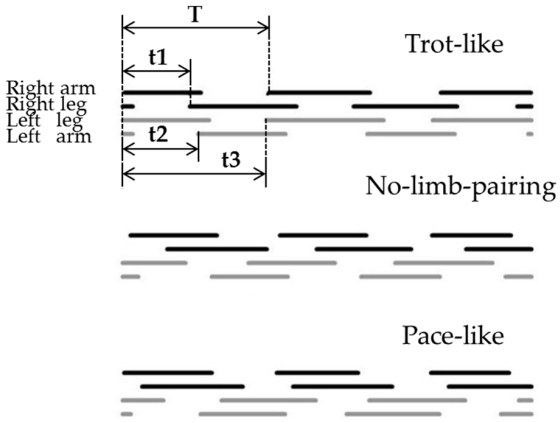

Figure 4. Three inter-limb coordination patterns of human crawling [6]. Solid lines represent the duration of stance phases and spaces represent the swing phases for each limb.

To explore the effect of crawling speed on the inter-limb coordination, limb phase lags at different speeds were calculated and analyzed in this study. In related studies, limb events like connection or separation were obtained by cameras [6,30], force sensors [31–33], or accelerometers [34–36]. In this study, ACC signals were used to detect the initiation of the stance phase of each limb and to calculate the ipsilateral phase lag, contralateral phase lag, and diagonal phase lag, since the contact or separation between the limbs and ground was accompanied by a sudden change of the acceleration of a certain limb.

$$IPL = \frac{t1}{T} \cdot 100\% \tag{5}$$

$$CPL = \frac{t2}{T} \cdot 100\% \tag{6}$$

$$DPL = \frac{t3}{T} \cdot 100\% \tag{7}$$

3. Results

3.1. Intra-Limb Muscle Coordination

Figure 5 shows the *VAF* values when 1 to 3 synergies were extracted from all 20 subjects at different speeds. When the threshold of *VAF* was set to 0.8, only one synergy could be extracted from each limb

for most subjects. Two synergies were obtained with *VAF* ranging from 90% to 95%, and three synergies could account for more than 95% of the variations. Synergies extracted from leg muscles accounted for more variations than those from arm muscles when the number of synergies was small, and as the number of synergies increased, these discrepancies decreased. Figure 6 illustrates an example of the muscle synergies extracted from the right arm of one subject. Two synergies (St_ra and Sw_ra) and their corresponding recruitment patterns (Cst_ra and Csw_ra) were extracted when the threshold of *VAF* was set to 0.9, and three synergies (Sa, Sb, and Sc) and their corresponding recruitment patterns (Ca, Cb, and Cc) were extracted when *VAF* was set to 0.95. From Ca and Cb, we found that synergies Sa and Sb were recruited approximately at the same time, and these two synergies could be considered as the fractions of St_ra. Since two muscle synergies accounted for more than 90 percent of the variations, two synergies were extracted from each limb for further analysis.

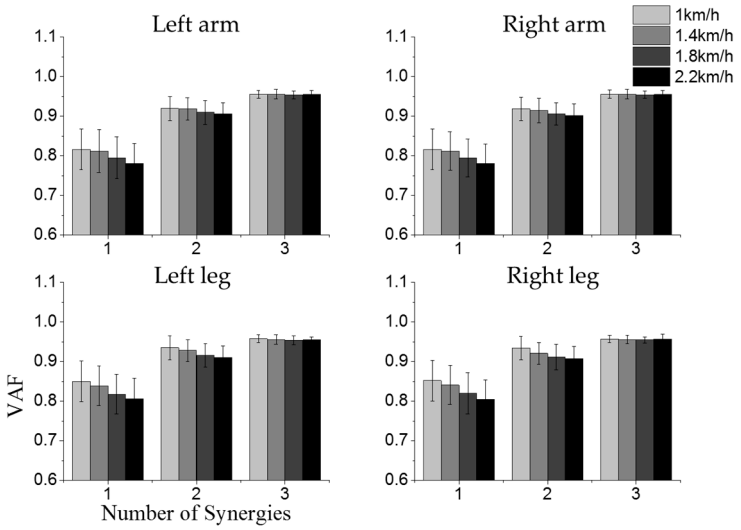

Figure 5. Statistics of the *VAF* values corresponding to different number of muscle synergies extracted from each limb (RA: right arm; LA: left arm; RL: right leg; LL: left leg) of all subjects under different speeds.

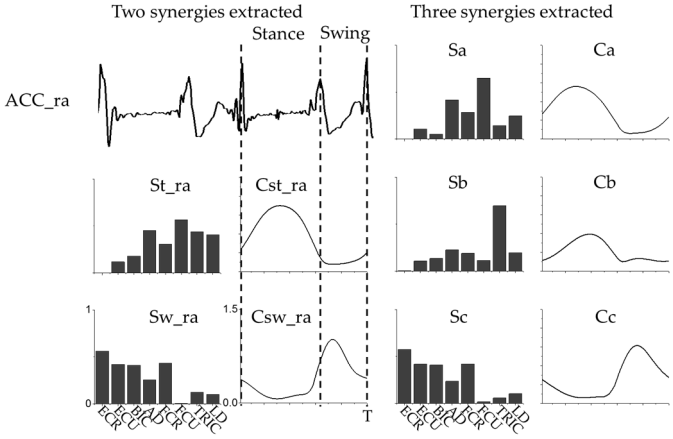

Figure 6. An example of muscle synergies extracted from the right arm of one subject. ACC_ra represents the acceleration data of the limb used to detect the stance and swing phase.

Using ACC signals, a whole cycle could be divided into the stance phase and swing phase for each limb (Figure 6). For all subjects, one of the two synergies (St_ra) extracted from the right arm muscle was mainly loaded by LD, TRIC, and FCU, and the corresponding recruitment pattern (Cst_ra)

was mainly activated at the stance phase. The other synergy (Sw_ra) was mainly loaded by BIC, ECU, and ECR, and was activated at the swing phase. So the main function of St_ra could be considered to support the upper trunk in a crawling cycle, and Sw_ra to swing the upper limb. On the other hand, one of the two synergy structures (St_rl) extracted from the leg muscles was dominated by GM, VM, and VL, whereas the other one (Sw_rl) was dominated by RA, ILIO, and RF. St_rl and Sw_rl played the same role as St_ra and Sw_ra. In the following analysis, synergies relating to the stance phase were named as St_ra (Cst_ra), St_la (Cst_la), St_rl (Cst_rl), and St_ll (Cst_ll), and synergies relating to the swing phase were named as Sw_ra (Csw_ra), Sw_la (Csw_la), Sw_rl (Csw_rl), and Sw_ll (Csw_ll) for the right arm, left arm, right leg, and left leg, respectively.

3.2. Inter-Limb Coordination

Taking subject AD7 as an example, Figure 7 demonstrates the typical sEMG envelopes during crawling cycles at different speeds. It could be observed from the figure that the activation levels of the upper limb muscles were significantly higher than those of the lower limb muscles. At the same time, muscle activation increased with the increase of the crawling speed. Figure 8 illustrates cycle duration, stance phase duration, and swing phase duration of each limb of all 20 subjects at different crawling speeds. As expected, the cycle duration decreased with crawling speed. From 1 km/h to 1.8 km/h, there was no significant change in the swing duration with the increase of speed. That is to say, the decrease of the cycle duration mainly resulted from the reduction of the stance duration. In addition, the swing duration was consistently shorter in the arms compared with the legs.

Figure 9 illustrates the effects of speed on the limb phase lags. Ipsilateral phase lags of all subjects ranged from 0.5 to 1. All subjects with no limb pairing crawled in a lateral-sequence pattern (IPL: 0.6–0.9). As shown in Figure 9, the change of speed failed to influence the contralateral phase lag ($p < 0.05$). That is to say, the coordination patterns between homologous limbs were not influenced by speed. However, ipsilateral phase lags and diagonal phase lags changed with speed for most subjects, and individual differences existed. Ipsilateral phase lags of subjects adopting a trot-like pattern (like AD17, AD19, and AD20) or pace-like pattern (like AD2 and AD4) at low speeds changed slightly at high speeds. Ipsilateral phase lag values of most subjects with no limb pairing (like AD7 and AD10) changed dramatically to 0.5 or 1 at high speeds. In other words, subjects with no-limb-pairing tended to adopt trot-like or pace-like patterns when crawling at high speeds.

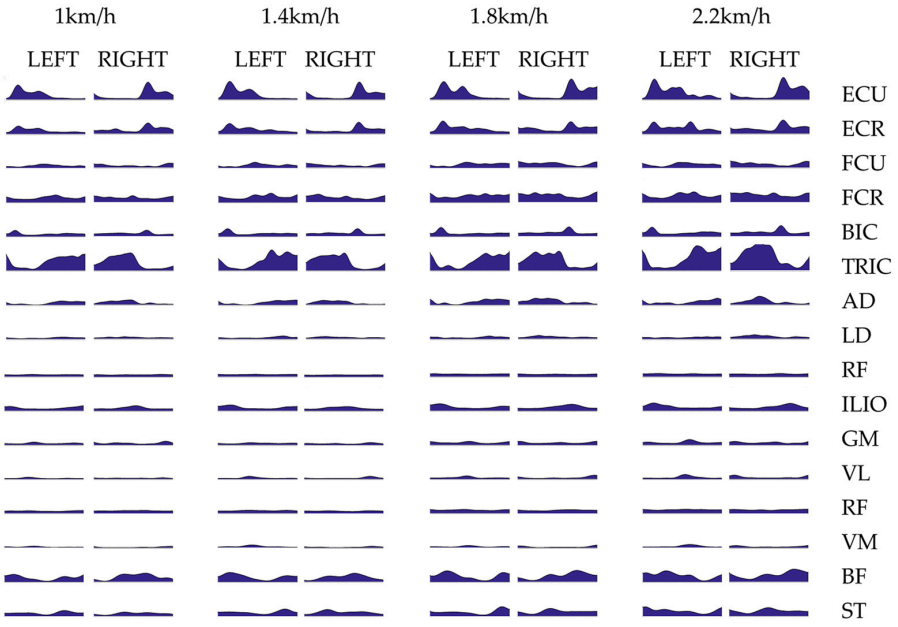

Figure 7. Illustration of the typical sEMG envelopes during crawling cycles at different speeds.

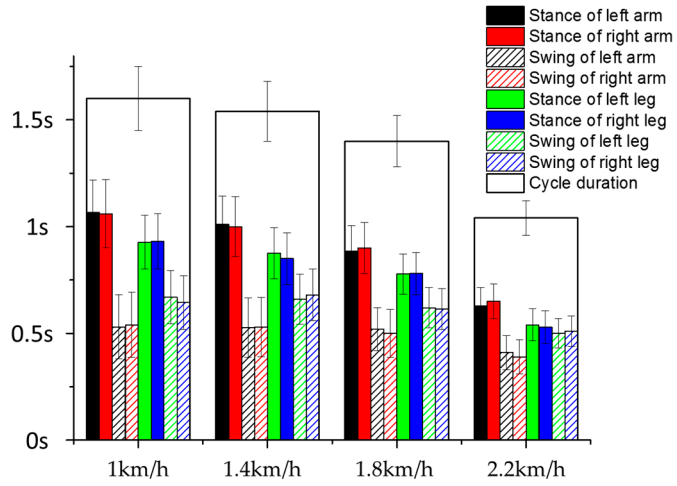

Figure 8. Cycle duration, stance phase duration, and swing phase duration (Mean ± SD) at different crawling speeds.

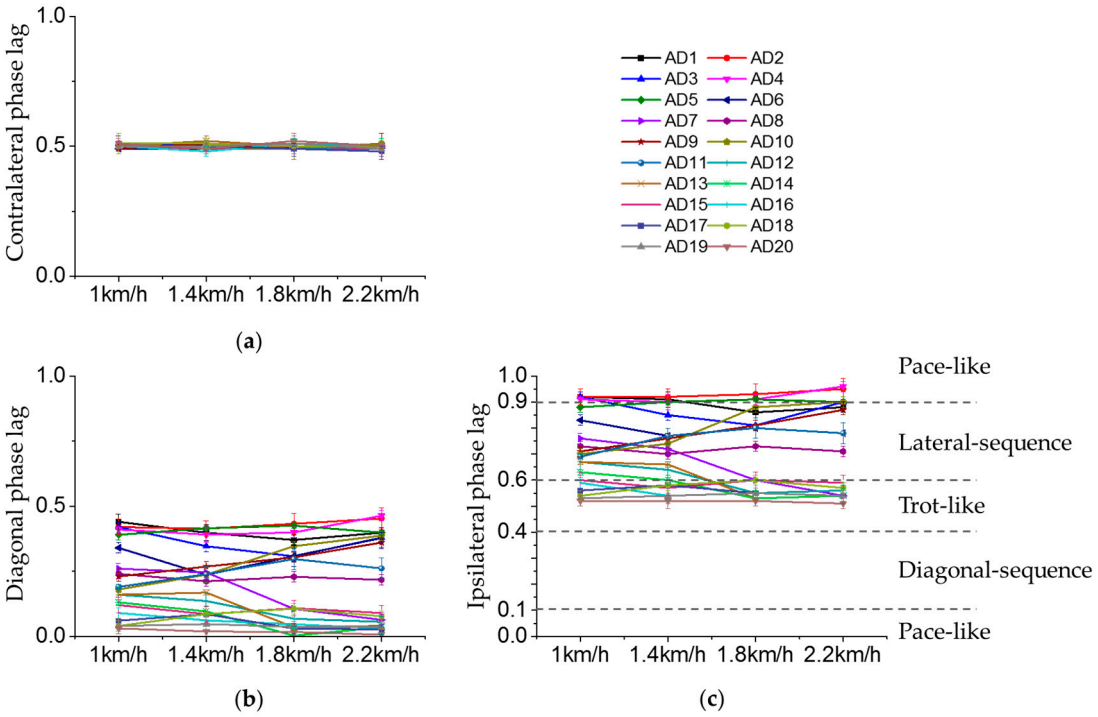

Figure 9. Limb phase lags at different speeds. (**a**) Contralateral phase lags; (**b**) Diagonal phase lags; (**c**) Ipsilateral phase lags.

In order to demonstrate the inter-limb coordination from the view of muscle synergy, Figure 10 illustrates muscle synergies extracted from the four limbs of all 20 subjects under the standard crawling condition (1 km/h). In each limb, the stance phase and swing phase alternated periodically, and the corresponding muscle synergies were recruited. Although individual differences existed, the synergy structures extracted from the left side were similar to the corresponding structures of the right side for all subjects ($r_{St\_la\sim St\_ra}$ = 0.85 ± 0.09, $r_{Sw\_la\sim Sw\_ra}$ = 0.87 ± 0.08, $r_{St\_ll\sim St\_rl}$ = 0.82 ± 0.12, $r_{Sw\_ll\sim Sw\_rl}$ = 0.83 ± 0.12). There were half cycle delays between the recruitments of two synergies of the left and right sides with similar structure. It could also be observed that subjects in different crawling patterns exhibited different recruitment orders of muscle synergies. Subjects in a pace-like pattern (4 subjects) recruited St_ra and St_rl (or Sw_ra and Sw_rl) simultaneously and subjects in a

trot-like pattern (5 subjects) recruited St_ra and Sw_rl (or Sw_ra and St_rl) simultaneously. For the pace-like pattern and trot-like pattern, high recruitment similarity existed in the same type of muscle synergies (stance phase related or swing phase related) between subjects as shown in Figure 10 and Table 1. However, subjects in no-limb-pairing mode (11 subjects) exhibited large discrepancies in the recruitments of lower limb muscle synergies (r = 0.12–0.21).

Table 1. Recruitment similarity of the same type of muscle synergies between subjects in the same inter-limb coordination pattern.

Pattern	r_{Cst_la}	r_{Cst_ra}	r_{Csw_la}	r_{Csw_ra}	r_{Cst_ll}	r_{Cst_rl}	r_{Csw_ll}	r_{Csw_rl}
Pace-like	0.89 ± 0.04	0.90 ± 0.03	0.87 ± 0.06	0.88 ± 0.05	0.83 ± 0.10	0.82 ± 0.10	0.80 ± 0.11	0.81 ± 0.13
No-limb-pairing	0.87 ± 0.05	0.89 ± 0.06	0.85 ± 0.09	0.87 ± 0.07	0.12 ± 0.74	0.14 ± 0.71	0.19 ± 0.66	0.21 ± 0.62
Trot-like	0.92 ± 0.04	0.93 ± 0.03	0.86 ± 0.05	0.88 ± 0.04	0.82 ± 0.11	0.80 ± 0.13	0.76 ± 0.19	0.78 ± 0.17

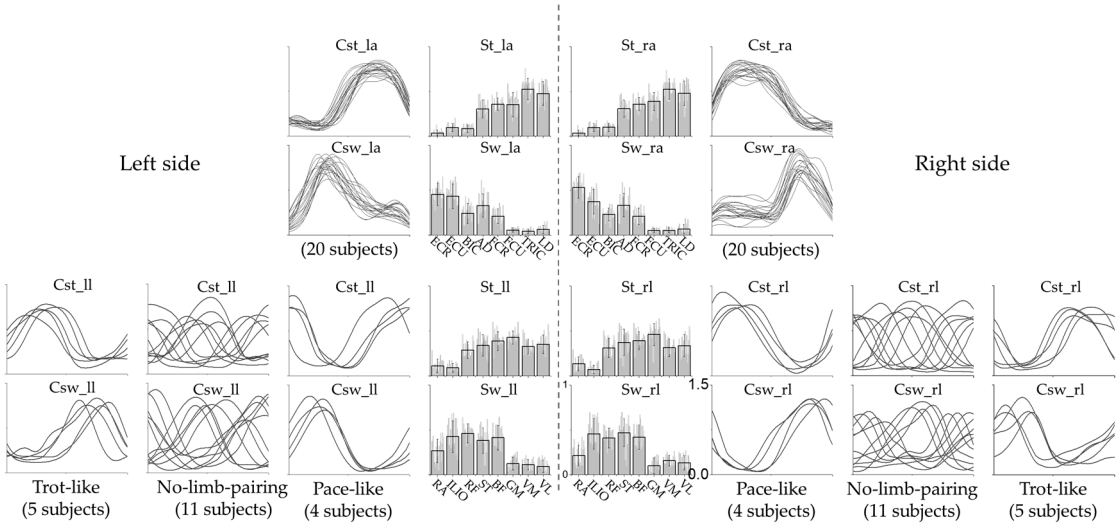

Figure 10. Synergy structures and recruitment patterns extracted from four limbs of all 20 subjects. Recruitment patterns of leg muscles are plotted separately according their inter-limb coordination patterns.

3.3. Effect of Crawling Speed on Intra- and Inter-Limb Coordination

From Figure 5, it could be observed that as the speed increased, the *VAF* remained similar when we chose to extract two synergies or more. Two synergies could account for more than 90 percent of the variations even at 2.2 km/h. When three synergies were extracted, the *VAF* values at different speeds were nearly the same and greater than 0.95. Therefore, two synergies were enough to account for the variations caused by the different crawling speeds.

Figure 11a illustrates the statistical features of the similarity coefficients between synergies extracted at different speeds other than 1 km/h (1.4, 1.8, and 2.2 km/h) and the speed of 1 km/h. Speed could influence the synergy structure as the between-group t-test indicated a significant difference in terms of the similarity coefficients. It could also be observed that the changes of the similarity coefficients relating to the stance phase (St_la, St_ra, St_ll, St_rl) were larger than those relating to the swing phase (Sw_la, Sw_ra, Sw_ll, Sw_rl). However, the effect of speed on the synergy structure was limited because the similarity coefficients between the synergy structures extracted under different speeds were all larger than 0.8. Figure 11b–d show the recruitment differences of synergies relating to the swing phase and stance phase under different speeds. The recruitment levels of all extracted synergies increased with the speed (Figure 11b), and the recruitment level changes of the synergies relating to the stance phase were much higher than those relating to the swing phase. Taking the combination of 2.2–1 km/h as an example, the Δp values of Cst_la, Cst_ra, Cst_ll, and Cst_rl increased more than 18 percent, but those of Csw_la, Csw_ra, Csw_ll, and Csw_rl increased less than 10 percent.

The phases of synergies relating to the swing phase advanced with the increase of the crawling speed but those of synergies relating to the stance phase remained almost unchanged (Figure 11c). The recruitment time lengths of all synergies were greatly affected by the speed (Figure 11d). As the treadmill sped up, the recruitment time lengths of synergies relating to the stance phase decreased but those of synergies relating to the swing phase increased.

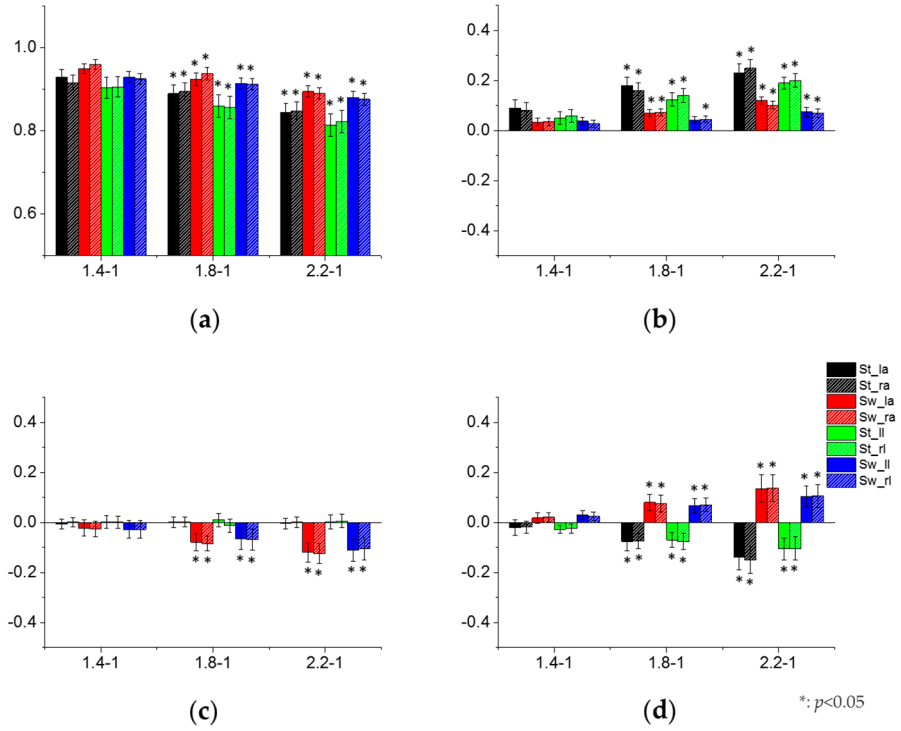

Figure 11. Effects of speed on (**a**) synergy structures and recruitment patterns of two similar synergies; (**b**) Recruitment level differences (Δp); (**c**) Recruitment phase lags (Δph); (**d**) Recruitment time length differences (Δtl). *T*-tests were performed between 1.8-1 and 1.4-1, and between 2.2-1 and 1.4-1, respectively. * means $p < 0.05$.

4. Discussion

Crawling can be seen as a kind of rhythmic motion. Some theories or models about the control mechanism of rhythmic locomotion in animals and humans were proposed in the past few decades. The concept of CPGs, which is considered to reside within the central nervous system and to control various rhythmic movements, was firstly proposed in 1911 [37]. In 1914, Graham and Brown built the "half center" model for CPG [38], suggesting that CPG controlled flexors and extensors alternately to achieve rhythmic locomotion. In 1981, Grillner proposed a new assumption of CPG organization. He thought that CPG was composed of several separate unit burst generators (UBG) controlling each joint of the limb and interacting with each other [39]. In 2006, Rybak and his coworkers suggested that the CPG was a two-level functional structure consisting of a half-center rhythm generator (RG) and a pattern formation (PF) circuit [40]. Although many models have been proposed and discussed, people still do not know exactly how rhythmic motions are generated and controlled. The potential advantages, disadvantages, and the plausibility of the UBG and two-level structure were debated widely in related studies [41–43]. Taking advantage of its great potential in revealing the motor control strategy of the CNS, muscle synergy analysis was adopted to explore the intra- and inter-limb muscle coordination of human hands-and-knees crawling under different speeds in this study, and the results can help to understand the underlying neuromuscular control mechanism of CNS on crawling movement.

4.1. The Possible CPG Model for Hands-and-Knees Crawling

Based on the intra-limb muscle coordination analysis in this study, two muscle synergies relating to the stance phase and swing phase were extracted from each limb. In addition, high structural similarity of muscle synergies was found among the subjects. This result is in accordance with previous studies of gait [18]. Therefore, we conclude that adult humans may share a common underlying muscle control mechanism of crawling. According to the theory of the half-center model, CPG controls the flexors and extensors alternately to achieve rhythmic locomotion [38]. One problem of the "half-center model" is that the real pattern of rhythmic movement is more complex, and some muscles are stimulated both in the flexion and the extension phases of a motion cycle [44]. In this study, some flexors and extensors were found to be grouped together and activated simultaneously. For example, in the stance phase of the right arm, AD, FCU, FCR, and TRIC were activated together. Moreover, some muscles such as AD and FCR contracted during both the stance phase and swing phase to achieve different functions. AD was responsible for stabilizing the shoulder in the stance phase, whereas in swing phase, AD propelled the arm. Therefore, we suppose that rhythmic locomotion in crawling movement is not produced by the alternating of flexors and extensors, but by the recruitment of task-oriented muscle synergies alternately, and one muscle can play roles in more than one muscle synergy.

The two-level CPG model suggests that the CPG is a two-level functional structure consisting of the half-center RG and PF circuit [40]. In this study, the results of the intra-limb coordination analysis conform to this model well. In each limb, the stance related synergy and swing related synergy coordinate with each other to achieve rhythmic movement. The PF network can be represented by synergy structures, and the RG can be exhibited by recruitment patterns. During crawling, RG in each limb may mediate the recruitment of the stance related synergy and swing related synergy to control one certain limb, and four limbs cooperate together to finish the crawling task.

4.2. Control Strategies of CNS to Crawling Speed

Considerable progress has been made toward the understanding of the commissural circuitry in the spinal cord that is responsible for the coordination of homologous (left and right) limbs (reviewed in [45]). In this study, the contralateral phase lag values never changed with crawling speed, implying that precise coordination existed between homologous limbs in crawling. As to the coordination of the ipsilateral limbs, the evidence in mammals suggests that CPGs in the cervical and lumbar spinal cord organize the hindlimb and forelimb locomotor activity during locomotion [37,46]. In this study, a large range of ipsilateral phase lag values were obtained from different subjects, suggesting that the temporal linkage between the recruitments of synergies extracted from arm muscles and leg muscles is flexible. In the meantime some subjects (such as AD7 and AD9) increased crawling speed by changing their crawling pattern from no-limb-pairing to pace-like or trot-like patterns. Similar results could be found in related studies [6,25]. The transition from no-limb-pairing to trot (or pace) is also similar to what has been observed in mice [47,48]. A recent computer model from the Rybak lab also exhibited the same transition [49]. These similarities hint at a similar underlying neural control.

The muscle synergy analysis of this study could reveal the control strategy of the CNS to adapt to the change of speed to a certain extent. On the one hand, the effect of speed on the synergy structure was found to be limited. This result indicated a good consistency of the synergy structure through different speeds in healthy adults and was consistent with the previous studies on gait [18,50]. On the other hand, human adults changed the recruitment levels, durations, and phases of the muscle synergies to adapt to the change of crawling speed. More concretely, the CNS shortened the cycle duration to adapt to high speed by decreasing the recruitment duration of stance related synergy and advancing the recruitment phase of swing related synergy. Moreover, with the increase of the crawling speed, the recruitment levels of synergies related to the stance phase increased more than those related to the swing phase. From the perspective of the two-level CPG model theory, the PF network is unchanged for a given motion task, and the CNS controls the crawling speed by modulating the rhythm generators of the four limbs.

4.3. Limitations and Future Work

Although this study explored the neuromuscular control strategy of crawling with hands and knees from the aspect of muscle synergy, there are a few limitations that await further study. Firstly, all the analyses were performed based on the two muscle synergies relating to the stance phase and swing phase, respectively. In this condition, the *VAF* threshold was set to 0.9 and the two major muscle synergies were extracted from each limb. However, as we know, more muscle synergies should be extracted when a higher *VAF* threshold is adopted. For example, the third muscle synergy would represent 5% of the variance when three synergies were extracted. The question of whether such minor muscle synergy is related to hands-and-knees crawling or only noise remains unsettled. Secondly, it is obvious that almost all trunk and limb muscles are involved in the crawling movement, which makes the crawling movement more complex than the gait. For example, erector spinae may play the role of stabilizing the whole body during crawling. In this study, only eight main limb related muscles from each limb were analyzed, which may hinder the exact understanding of the strategy of how the nervous system organizes the movement of the whole body. In future work, these muscles would be considered in more detail. Thirdly, muscle synergies were extracted from each limb separately, so inter-limb synergies may be overshadowed. For example, to remain stable, the muscles of different limbs may communicate with each other and commonly exhibit an extra synergy. Finally, although the research results corroborate the two-level CPG model, the influence of descending signals from higher centers and peripheral afferent feedback were not directly measured in this study.

5. Conclusions

In this study, the intra- and inter-limb muscle coordination in human hands-and-knees crawling movement were investigated by means of muscle synergy analysis. The intra-limb coordination was found to be relatively stable during human hands-and-knees crawling. Two synergies, one relating to the stance phase and the other relating to the swing phase, were extracted from each limb during a crawling cycle. With limited variations in structures, human adults changed the recruitment levels, durations, and phases of muscle synergies to adapt to the change of crawling speed. The inter-limb coordination changed with speed for most subjects, and subjects with no-limb-pairing tended to adopt the trot-like or pace-like pattern at high speeds. The research results of this study could be well explained by the two-level CPG model consisting of a half-center RG and a PF circuit.

Acknowledgments: This work was supported by the National Nature Science Foundation of China (grant numbers: 61671417 and 61431017).

Author Contributions: Xiaocong Niu analyzed the data, interpreted the results, and wrote the draft of the manuscript; Xiang Chen performed all stages of the study including data collection, analysis, interpretation, and substantial revision of the manuscript; De Wu participated in data collection and provided guidance to data analysis; Yi Yu and Xu Zhang participated in data analysis and revised the manuscript. All authors have read and approved the final version of the manuscript.

Conflicts of Interest: The authors declare that there is no conflict of interest including financial, consultant, institutional, and other relationships that might lead to bias or a conflict of interest.

References

1. McGraw, M.B. Neural maturation as exemplified in the changing reactions of the infant to pin prick. *Child Dev.* **1941**, *12*, 31–42. [CrossRef]
2. Adolph, K.E.; Vereijken, B.; Denny, M.A. Learning to crawl. *Child Dev.* **1998**, *69*, 1299–1312. [CrossRef] [PubMed]
3. Hildebrand, M. Symmetrical gaits of primates. *Am. J. Phys. Anthropol.* **1967**, *26*, 119. [CrossRef]
4. Hildebrand, M. Symmetrical gait of horses. *Science* **1965**, *150*, 701–708. [CrossRef] [PubMed]
5. Hildebrand, M. Analysis of tetrapod gaits: General considerations and symmetrical gaits. *Neural Control Locomot.* **1976**, *18*, 203–206. [CrossRef]

6. Patrick, S.K.; Noah, J.A.; Yang, J.F. Interlimb coordination in human crawling reveals similarities in development and neural control with quadrupeds. *J. Neurophysiol.* **2009**, *101*, 603–613. [CrossRef] [PubMed]
7. MacLellan, M.J.; Ivanenko, Y.P.; Catavitello, G.; La Scaleia, V.; Lacquaniti, F. Coupling of upper and lower limb pattern generators during human crawling at different arm/leg speed combinations. *Exp. Brain Res.* **2013**, *225*, 217–225. [CrossRef] [PubMed]
8. Tan, U.; Derawi, M.O.; Bours, P.; Holien, K. Quadrupedal locomotor characteristics of uner tan syndrome cases, healthy humans, and nonhuman primates in evolutionary perspectives improved cycle detection for accelerometer based gait authentication. In Proceedings of the 2010 Sixth International Conference on Intelligent Information Hiding and Multimedia Signal Processing, Darmstadt, Germany, 15–17 October 2010.
9. Righetti, L.; Nylen, A.; Rosander, K.; Iispeert, A.J. Kinematic and gait similarities between crawling human infants and other quadruped mammals. *Front. Neurol.* **2015**, *6*, 17. [CrossRef] [PubMed]
10. Ting, L.H.; McKay, J.L. Neuromechanics of muscle synergies for posture and movement. *Curr. Opin. Neurobiol.* **2007**, *17*, 622–628. [CrossRef] [PubMed]
11. Danner, S.M.; Hofstoetter, U.S.; Freundl, B.; Binder, H.; Mayr, W.; Rattay, F.; Minassian, K. Human spinal locomotor control is based on flexibly organized burst generators. *Brain* **2015**, *138*, 577–588. [CrossRef] [PubMed]
12. D'Avella, A.; Saltiel, P.; Bizzi, E. Combinations of muscle synergies in the construction of a natural motor behavior. *Nat. Neurosci.* **2003**, *6*, 300–308. [CrossRef] [PubMed]
13. Ting, L.H.; Macpherson, J.M. A limited set of muscle synergies for force control during a postural task. *J. Neurophysiol.* **2005**, *93*, 609–613. [CrossRef] [PubMed]
14. Meyer, A.J.; Eskinazi, I.; Jackson, J.N.; Rao, A.V.; Patten, C.; Fregly, B.J. Muscle synergies facilitate computational prediction of subject-specific walking motions. *Front. Bioeng. Biotechnol.* **2016**, *4*, 77. [CrossRef] [PubMed]
15. Chvatal, S.A.; Ting, L.H. Voluntary and reactive recruitment of locomotor muscle synergies during perturbed walking. *J. Neurosci.* **2012**, *32*, 12237–12250. [CrossRef] [PubMed]
16. Ivanenko, Y.P.; Poppele, R.E.; Lacquaniti, F. Five basic muscle activation patterns account for muscle activity during human locomotion. *J. Physiol.* **2004**, *556*, 267–282. [CrossRef] [PubMed]
17. Dominici, N.; Ivanenko, Y.P.; Cappellini, G.; D'Avella, A.; Mondi, V.; Cicchese, M.; Fabiano, A.; Silei, T.; Di Paolo, A.; Giannini, C.; et al. Locomotor Primitives in Newborn Babies and Their Development. *Science* **2011**, *334*, 997–999. [CrossRef] [PubMed]
18. Tang, L.; Li, F.; Cao, S.; Zhang, X.; Wu, D.; Chen, X. Muscle synergy analysis in children with cerebral palsy. *J. Neural Eng.* **2015**, *12*, 46017. [CrossRef] [PubMed]
19. Chia, B.N.; Pedrocchi, A.; Nardone, A.; Schieppati, M.; Baccinelli, W.; Monticone, M.; Ferrigno, G.; Ferrante, S. Tuning of muscle synergies during walking along rectilinear and curvilinear trajectories in humans. *Ann. Biomed. Eng.* **2017**, *45*, 1204–1218. [CrossRef] [PubMed]
20. Hermens, H.J.; Freriks, B.; Disselhorst-Klug, C.; Rau, G. Development of recommendations for SEMG sensors and sensor placement procedures-Journal of Electromyography and Kinesiology. *J. Electromyogr. Kinesiol.* **2000**, *10*, 361–374. [CrossRef]
21. Boettcher, C.E.; Ginn, K.A.; Cathers, I. Standard maximum isometric voluntary contraction tests for normalizing shoulder muscle EMG. *J. Orthop. Res.* **2008**, *26*, 1591–1597. [CrossRef] [PubMed]
22. Barr, A.E.; Goldsheyder, D.; Ozkaya, N.; Nordin, M. Testing apparatus and experimental procedure for position specific normalization of electromyographic measurements of distal upper extremity musculature. *Clin. Biomech.* **2001**, *16*, 576–585. [CrossRef]
23. Veragarcia, F.J.; Moreside, J.M.; Mcgill, S.M. MVC techniques to normalize trunk muscle EMG in healthy women. *J. Electromyogr. Kinesiol.* **2010**, *20*, 10–16. [CrossRef] [PubMed]
24. Rouffet, D.M.; Hautier, C.A. EMG normalization to study muscle activation in cycling. *J. Electromyogr. Kinesiol.* **2008**, *18*, 866–878. [CrossRef] [PubMed]
25. Gallagher, S.; Pollard, J.; Porter, W.L. Locomotion in restricted space: Kinematic and electromyographic analysis of stoopwalking and crawling. *Gait Posture* **2011**, *33*, 71–76. [CrossRef] [PubMed]
26. Lee, D.D.; Seung, H.S. Learning the parts of objects by non-negative matrix factorization. *Nature* **1999**, *401*, 788–791. [CrossRef] [PubMed]
27. Huang, C.; Chen, X.; Cao, S.; Zhang, X. Muscle-tendon units localization and activation level analysis based on high-density surface EMG array and NMF algorithm. *J. Neural Eng.* **2016**, *13*, 066001. [CrossRef] [PubMed]

28. Winter, D.A.; Yack, H.J. EMG profiles during normal human walking: Stride-to-stride and inter-subject variability. *Electroencephalogr. Clin. Neurophysiol.* **1987**, *67*, 402–411. [CrossRef]
29. Clark, D.J.; Ting, L.H.; Zajac, F.E.; Neptune, R.R.; Kautz, S.A. Merging of healthy motor modules predicts reduced locomotor performance and muscle coordination complexity post-stroke. *J. Neurophysiol.* **2010**, *103*, 844–857. [CrossRef] [PubMed]
30. Ivanenko, Y.P.; Poppele, R.E.; Lacquaniti, F. Spinal cord maps of spatiotemporal alpha-motoneuron activation in humans walking at different speeds. *J. Neurophysiol.* **2006**, *95*, 602–618. [CrossRef] [PubMed]
31. Maclellan, M.J.; Ivanenko, Y.P.; Cappellini, G.; Sylos, L.F.; Lacquaniti, F. Features of hand-foot crawling behavior in human adults. *J. Neurophysiol.* **2012**, *107*, 114–125. [CrossRef] [PubMed]
32. Arsenault, A.B.; Winter, D.A.; Marteniuk, R.G. Is there a 'normal' profile of EMG activity in gait? *Med. Biol. Eng. Comput.* **1986**, *24*, 337–343. [CrossRef] [PubMed]
33. Dietz, V.; Fouad, K.; Bastiaanse, C.M. Neuronal coordination of arm and leg movements during human locomotion. *Eur. J. Neurosci.* **2001**, *14*, 1906–1914. [CrossRef] [PubMed]
34. Derawi, M.O.; Bours, P.; Holien, K. Improved cycle detection for accelerometer based gait authentication. In Proceedings of the Sixth International Conference on Intelligent Information Hiding and Multimedia Signal Processing (IIH-MSP), Darmstadt, Germany, 15–17 October 2010; pp. 312–317. [CrossRef]
35. Takeda, R.; Tadano, S.; Todoh, M.; Morikawa, M.; Nakayasu, M.; Yoshinari, S. Gait analysis using gravitational acceleration measured by wearable sensors. *J. Biomech.* **2009**, *42*, 223–233. [CrossRef] [PubMed]
36. Lau, H.; Tong, K. The reliability of using accelerometer and gyroscope for gait event identification on persons with dropped foot. *Gait Posture* **2008**, *27*, 248–257. [CrossRef] [PubMed]
37. Brown, T.G. The intrinsic factors in the act of progression in the mammal. *Proc. R. Soc. Lond. B Biol. Sci.* **1911**, *84*, 308–319. [CrossRef]
38. Graham, B.T. On the nature of the fundamental activity of the nervous centres; together with an analysis of the conditioning of rhythmic activity in progression, and a theory of the evolution of function in the nervous system. *J. Physiol.* **1914**, *48*, 18–46. [CrossRef]
39. Grillner, S. Control of locomotion in bipeds, tetrapods, and fish. *Compr. Physiol.* **2011**. [CrossRef]
40. Rybak, I.A.; Shevtsova, N.A.; Lafreniere-Roula, M.; McCrea, D.A. Modelling spinal circuitry involved in locomotor pattern generation: Insights from deletions during fictive locomotion. *J. Physiol.* **2006**, *577*, 617–639. [CrossRef] [PubMed]
41. Hagglund, M.; Dougherty, K.J.; Borgius, L.; Itohara, S.; Iwasato, T.; Kiehn, O. Optogenetic dissection reveals multiple rhythmogenic modules underlying locomotion. *Proc. Natl. Acad. Sci. USA* **2013**, *110*, 11589–11594. [CrossRef] [PubMed]
42. Grillner, S.; El Manira, A. The intrinsic operation of the networks that make us locomote. *Curr. Opin. Neurobiol.* **2015**, *31*, 244–249. [CrossRef] [PubMed]
43. McLean, D.L.; Dougherty, K.J. Peeling back the layers of locomotor control in the spinal cord. *Curr. Opin. Neurobiol.* **2015**, *33*, 63–70. [CrossRef] [PubMed]
44. Rossignol, S. Neural control of stereotypic limb movements. *Compr. Physiol.* **1996**. [CrossRef]
45. Kiehn, O. Locomotor circuits in the mammalian spinal cord. *Annu. Rev. Neurosci.* **2006**, *29*, 279–306. [CrossRef] [PubMed]
46. Grillner, S.; Zangger, P. On the central generation of locomotion in the low spinal cat. *Exp. Brain Res.* **1979**, *34*, 241–261. [CrossRef] [PubMed]
47. Mendes, C.S.; Bartos, I.; Márka, Z.; Akay, T.; Márka, S.; Mann, R.S. Quantification of gait parameters in freely walking rodents. *BMC Biol.* **2015**, *13*, 50. [CrossRef] [PubMed]
48. Bellardita, C.; Kiehn, O. Phenotypic characterization of speed-associated gait changes in mice reveals modular organization of locomotor networks. *Curr. Biol.* **2015**, *25*, 1426–1436. [CrossRef] [PubMed]
49. Danner, S.M.; Wilshin, S.D.; Shevtsova, N.A.; Rybak, I.A. Central control of interlimb coordination and speed-dependent gait expression in quadrupeds. *J. Physiol.* **2016**, *594*, 6947–6967. [CrossRef] [PubMed]
50. Monaco, V.; Ghionzoli, A.; Micera, S. Age-related modifications of muscle synergies and spinal cord activity during locomotion. *J. Neurophysiol.* **2010**, *104*, 2092–2102. [CrossRef] [PubMed]